Anisotropy of biotite-rich rock: Non-ellipticity of the *P*-velocity and singularity of the *S*-velocity

Osamu Nishizawa(1), Kyuichi Kanagawa(2), Takashi Yoshino(3), Mamoru Takanashi(4), and Kentaro Yasunaga(2)

(1)*Geological Survey of Japan,* (2)*Faculty of Science, Chiba University,* (3)*Department Civil and Environmental Engineering, Toyo University,* (4)*Japan National Oil Coporation*

Abstract

We made laboratory measurements of velocity anisotropy of biotite schist from Hidaka metamorphic belt, Hokkaido, Japan, under confining pressures up to 150 MPa, and interpreted the measured velocity anisotropy by employing a crack model proposed by Nishizawa (1982). The biotite schist shows foliation plane and lineation in the foliation plane. The crystallographic layer of biotite and the crack planes are mostly align parallel to the foliation plane. Anisotropy of the rock is basically transverse isotropy (TI) with the symmetry axis perpendicular to the foliation. The crack model treats cracks as oblate spheroid inclusions, and cracks are inserted into an initially anisotropic matrix having TI symmetry with all the crack normal parallel to the symmetry axis. Then the overall elastic properties of the crack-containing rock also show TI. The crack model suggests that the changes of the P- and S-velocities under pressure can be interpreted as closure of aligned cracks under pressure. Comparing the calculated phase velocities of P- and S-waves with the phase velocities obtained from Thomsen's approximation, we found that Thomsen's approximations are applicable for P- and SH-waves for most of the cases. However, for the phase velocity of SV-wave, Thomsen's approximation shows considerable discrepancy against exact velocity values when crack density is large or when cracks are filled with gas.

Introduction

It is well known that oriented cracks produce velocity anisotropy. If all cracks are aligned in the same direction in an isotropic rock, the overall elastic properties of the rock show transverse isotropy (TI) where the P- and S- velocities are rotationally symmetric. Velocity anisotropy is mainly controlled by crack shape: thin cracks produce strong velocity anisotropy. On the other hand, some rocks have an intrinsic velocity anisotropy caused by the lattice-preferred orientation (LPO) of anisotropic minerals. When rock anisotropy is produced by both oriented cracks and LPO of anisotropic minerals, the rock is modeled as a composite that contains oriented cracks in an anisotropic medium. Nishizawa (1982) presented a method to calculate velocity anisotropy caused by aligned cracks in an anisotropic matrix. This method is based on calculation of the Eshelby's tensor in an anisotropic medium. The integral given by Lin and Mura (1973) provides the Eshelby's tensor by numerical calculations, and overall elastic properties of the crack-containing rock can be obtained by using the calculated Eshelby tensor. This approach has been used for interpreting VSP (Vertical Seismic Profiling) data (Douma & Crampin, 1990), or for modeling the velocity anisotropy of shale (Hornby et al., 1994). The same approach has been employed by Singh et al. (2000), where they showed a possibility of unique S-velocity anisotropy produced by melt inclusions in the inner core of the Earth.

Recently, Nishizawa and Yoshino (2000) extended Nishizawa's approach to calculate velocity anisotropy of mica-rich rocks. In their treatment, mica minerals are inserted into an initially isotropic matrix with their crystallographic axes aligned in the same direction. Since elastic anisotropy of mica mineral can be treated as TI symmetry, the overall elastic properties of rock also show TI. Biotite-rich rocks show a bulge of the SV-wave phase velocity surface. This produces a line singularity of S-wave, where SV- and SH-wave phase velocity surfaces intersect each other (Crampin & Yedlin, 1981). The results of the inclusion model well explain the laboratory-measured intrinsic velocity anisotropy in biotite-rich schist (Takanashi et al., 2000).

Here, we model crack-containing biotite-rich rocks by using the same approach of Nishizawa (1982) or Nishizawa and Yoshino (2000), where aligned oblate spheroidal cracks are distributed in an anisotropic matrix of TI symmetry. We will present velocity anisotropy of the crack-containing biotite-rich rock and compare the calculated anisotropy with the laboratory velocity measurements under confining pressures, where cracks are closed with increasing the confining pressure.

Inclusion model

To estimate the overall elastic constants of crack-containing medium, we use the Eshelby's composite medium model consisting of matrix and inclusion, and calculate change of the elastic energy due to inclusions. Elastic constants (or compliance constants) are given by differentiation of elastic energy with respect to strain (or stress).

We consider that the matrix material has homogeneous strain, e_{ij}^{A}, or stress, σ_{ij}^{A}. When an inclusion appears inside the matrix, the composite medium becomes an internal stress state. We regard the composite as an equivalent homogeneous medium, and estimate elastic energy corresponding to the equivalent strain, e^{A}_{ij}, or stress, σ^{A}_{ij}. To calculate the elastic energy change due to inclusions (cracks), Eshelby (1957) introduced stress-free strain e^{T}_{ij} (also called eigen strain; Lin and Mura, 1973).

In energy calculation, there are two conditions defined at the far field of the composite medium: constant applied force and constant displacements (Eshelby, 1957; Yamamoto et al., 1981; Nishizawa, 1982). For calculating the energy of composite medium, Eshelby (1957) presented an idea that replaces the inclusion with matrix material and gives a fictitious stress-free strain inside the inclusion. He demonstrated that the change of the elastic energy corresponding to the equivalent strain e^{A}_{ij} or stress σ^{A}_{ij} is given by the fictitious stress-free strain e^{T}_{ij} as

$$\Delta E = \mp(1/2)\sigma^{\mathrm{A}}_{ij} e^{\mathrm{T}}_{ij}\phi \ , \tag{1}$$

where the sign $\mp$ denotes the two conditions: constant external force and constant surface displacements, respectively. ϕ is the volume fraction of inclusions. σ^{A}_{ij} is related to homogeneous strain through elastic constants of the matrix c^0_{ijkl} as $\sigma^{\mathrm{A}}_{ij} = c^0_{ijkl} e^{\mathrm{A}}_{kl}$.

Eshelby (1957) derived a relationship between the fictitious stress-free strain e^{T}_{ij} and strain in homogeneous matrix e^{A}_{ij}. Let c'_{ijkl} be the elastic constants of the inclusion. The relation between e^{A}_{ij} and e^{T}_{ij} is given by using Eshelby's tensor, S_{ijkl}.

$$c^0_{ijkl} e^{\mathrm{T}}_{kl} = \Delta c_{ijkl} e^{\mathrm{A}}_{kl} + \Delta c_{ijkl} S_{klmn} e^{\mathrm{T}}_{mn} \ , \tag{2}$$

where Δc_{ijkl} is the difference of the elastic constants between matrix and inclusion:

$$\Delta c_{ijkl} = c^0_{ijkl} - c'_{ijkl} \ . \tag{3}$$

Equation (2) shows that the fictitious stress-free strain e^{T}_{ij} can be obtained by strain of the matrix material e^{A}_{ij}, Eshelby's tensor S_{ijkl}, and the elastic constants of matrix and inclusion, c^0_{ijkl} and c'_{ijkl}. In crack problems, c'_{ijkl} is given by bulk modulus of fluid (gas or liquid). When the matrix is TI, Eshelby's tensor S_{ijkl} can be calculated by numerical integrations given by Lin and Mura (1973) (Nishizawa, 1982; Douma, 1988).

The composite is regarded as an equivalent homogeneous medium and its elastic energy is given by the following equations, corresponding to the conditions shown in equation (1):

$$\frac{1}{2}{c^*_{ijkl}}^{-1}\sigma^{\mathrm{A}}_{ij}\sigma^{\mathrm{A}}_{kl} = \frac{1}{2}{c^0_{ijkl}}^{-1}\sigma^{\mathrm{A}}_{ij}\sigma^{\mathrm{A}}_{kl} + \frac{1}{2}\sigma^{\mathrm{A}}_{ij}e^{\mathrm{T}}_{ij}\phi \ , \tag{4}$$

$$\frac{1}{2}c^*_{ijkl}e^{\mathrm{A}}_{ij}e^{\mathrm{A}}_{kl} = \frac{1}{2}c^0_{ijkl}e^{\mathrm{A}}_{ij}e^{\mathrm{A}}_{kl} - \frac{1}{2}\sigma^{\mathrm{A}}_{ij}e^{\mathrm{T}}_{ij}\phi \ . \tag{5}$$

where c^*_{ijkl} denotes elastic constants of the equivalent homogeneous medium, and ${c^*_{ijkl}}^{-1}$ and ${c^0_{ijkl}}^{-1}$ denote the inverse of the matrices c^*_{ijkl} and c^0_{ijkl}, respectively. The energy given by equation (4) or (5) is valid only when ϕ is very small. Therefore, we start from the initial inclusion-free matrix and repeat calculation with a small increment of inclusion volume $\Delta\phi$, regarding the composite of the previous step as an equivalent homogeneous matrix material. This is called Differential Equivalent Medium Method (DEM) or Numerical Self Consistent Approach (NSC) (Le Ravalec and Gueguen, 1996a, b; Yamamoto, 1981). The equations are given by

$$\frac{1}{2}{c^{*(n)}_{ijkl}}^{-1}\sigma^{\mathrm{A}(n-1)}_{ij}\sigma^{\mathrm{A}(n-1)}_{ij} = \frac{1}{2}{c^{0(n-1)}_{ijkl}}^{-1}\sigma^{\mathrm{A}(n-1)}_{ij}\sigma^{\mathrm{A}(n-1)}_{kl} + \frac{1}{2}\sigma^{\mathrm{A}(n-1)}_{ij}e^{\mathrm{T}(n-1)}_{ij}\Delta\phi \ , \tag{6}$$

$$\frac{1}{2}c^{*(n)}_{ijkl}e^{\mathrm{A}(n-1)}_{ij}e^{\mathrm{A}(n-1)}_{ij} = \frac{1}{2}c^{0(n-1)}_{ijkl}e^{\mathrm{A}(n-1)}_{ij}e^{\mathrm{A}(n-1)}_{kl} - \frac{1}{2}\sigma^{\mathrm{A}(n-1)}_{ij}e^{\mathrm{T}(n-1)}_{ij}\Delta\phi \ , \tag{7}$$

where $c^{*(n)}_{ijkl}$ and ${c^{*(n)}_{ijkl}}^{-1}$ are the elastic constants and its inverse (compliance) obtained at the nth step of calculation, respectively, and the superscripts $(n-1)$ of c^0_{ijkl}, e^{A}_{ij}, σ^{A}_{ij} and e^{T}_{ij} denote the values of $(n-1)$th step. $e^{\mathrm{T}(n-1)}_{ij}$ is given by Eshlby's tensor for the effective homogeneous medium at the $(n-1)$th step. DEM evaluates the stress or strain change inside the composite medium by assuming the composite medium as a new homogeneous matrix with new elastic constants.

Numerical calculation

Elastic constants of anisotropic rock

To calculate elastic constants of the crack-containing biotite-rich rock, we must calculate elastic properties of the matrix medium. First we consider a biotite-rich rock consisting of isotropic matrix and 30 % volume fraction of biotite. We assume the elastic constants of the isotropic matrix as λ = μ = 35 GPa. Biotite is a monoclinic crystal, but it can be treated as a hexagonal crystal having the elastic constants shown in Table 1 (Alekesandrov & Ryzhova, 1961) by assuming the symmetry axis perpendicular to the crystallographic layered sheet.

Table. 1

	C_{11}	C_{33}	C_{44}	C_{66}	C_{13}
biotite	186.0	54.0	5.8	76.8	11.6

Hereafter, we use the Voigt notation C_{ij} for denoting the measured and calculated values, instead of the notation used in theoretical formulations, c_{ijkl}. Note that $C_{12} = C_{11} - 2C_{66}$. Nishizawa & Yoshino (2000) pointed out that the crystal shape of biotite controls velocity anisotropy of biotite-rich rocks. Since biotite usually appears as thin crystals, its shape is assumed as an oblate spheroid with the major axis a and the minor axis c. The crystal shape is expressed by the aspect ratio $\alpha = c/a$ Table 2 is the elastic constants of the biotite-rich rock for the biotite crystal aspect ratio 1/20, which are used as elastic constants of the rock matrix.

Table. 2

	C_{11}	C_{33}	C_{44}	C_{66}	C_{13}
rock matrix	126.6	81.9	15.8	47.0	24.4

Next, we assume that the crack-free biotite-rich rock as a homogeneous matrix and insert aligned micro cracks into the matrix. In each step of the calculation, we have two elastic constants calculated from the equations (6) and (7). The difference between two elastic constants becomes large as the difference of elastic constants between inclusion and matrix becomes large. The difference is also controlled by crack aspect ratio. We selected a small $\Delta\phi$ value for a small crack aspect ratio, and calculate the average obtained from (6) and (7).

Thomsen's anisotropic parameter

In TI media, P- and S-waves are expressed as qP, qSV and SH in exact notations. However we use simple notations P, SV and SH, because those waves are clearly distinguished in TI media, and cause no confusion. SV-wave is polarizes in the plane containing the symmetry axis, whereas SH-wave polarizes in the plane perpendicular to the symmetry axis. When anisotropy of TI is weak, phase velocities in the direction θ (an angle measured form the symmetry axis) are given by Thomsen's anisotropic parameters and the P- and S-velocities along the symmetry axis, $V_P(0)$ and $V_S(0)$.

$$V_P(\theta) = V_P(0)(1 + \delta \sin^2\theta \cos^2\theta + \epsilon \sin^4\theta), \quad (8)$$

$$V_{SV}(\theta) = V_S(0)(1 + \sigma \sin^2\theta \cos^2\theta) \ , \quad (9)$$

$$V_{SH}(\theta) = V_S(0)(1 + \gamma \sin^2\theta) \ , \quad (10)$$

where ϵ, γ and δ are defined by elastic constants or approximated by the velocity values θ= 0, $\pi/2$ and $\pi/4$:

$$\epsilon = \frac{C_{11} - C_{33}}{2C_{33}} \approx \frac{V_P(\pi) - V_P(0)}{V_P(0)} \ , \quad (11)$$

$$\gamma = \frac{C_{66} - C_{44}}{2C_{44}} \approx \frac{V_{SH}(\pi) - V_{SH}(0)}{V_{SH}(0)} \quad , \quad (12)$$

$$\delta = \frac{(C_{13} + C_{44})^2 - (C_{33} - C_{44})^2}{2C_{13}(C_{33} - C_{44})} \approx 4\left[\frac{V_P(\pi/4)}{V_P(0)} - 1\right] - \left[\frac{V_P(\pi/2)}{V_P(0)} - 1\right] \quad , \quad (13)$$

and σ is given by

$$\sigma = \left(\frac{V_P(0)}{V_S(0)}\right)^2 (\epsilon - \delta) \ . \quad (14)$$

The phase velocity surface of SV-wave show a bulge around $\theta = \pi/4$ depending on the value of σ. We examine applicability of Thomsen's approximation by comparing the approximate velocities with the exact velocities.

Phase velocity surface

For calculating phase velocity, we assume the rock density as 2.75 $\times$ 10^3 kg/m^3. Fig. 1 a-d show phase velocity surfaces of P-, SV- and SH-waves projected on the section including the symmetry axis.

We assume thin cracks with aspect ratio 0.01 filled with fluid. The bulk modulus of the crack-filling fluid controls anisotropy. We change fluid bulk modulus K_f from 0.01 to 1 GPa. The large and small values of bulk modulus correspond to the cracks filled with liquid or gas, respectively. (a) and (b) show the phase velocity surface of P-wave for the crack densities 0.02 and 0.06. Thomsen's approximation and the velocity of the crack-free rock are also shown in the same figure. (c) and (d) show the phase velocity surface of SV- and SH-waves for the same fluid bulk modulus, corresponding to crack densities 0.02 and 0.06, respectively. (e)-(h) are the phase velocity surfaces for the fluid bulk modulus 1 GPa: (e) and (f) are the P-velocity for crack density 0.02 and 0.06, respectively, and (g) and (h) are the SV- and SH-velocities for crack densities 0.02 and 0.06, respectively. We calculate Thomsen's anisotropic parameters from the P- and S-velocities in the axial directions and from the P-velocity in the direction θ=π/4, because velocity values are the primary data of the field observations. For the most cases of the P- and SH- velocities, Thomsen's approximation agrees fairly well with the exact velocity values calculated from elastic constants of the cracked rock. However, when crack density is small or the fluid bulk modulus is large, Thomsen's approximation underestimates the SV-velocity in the range $\theta < \pi/4$, and overestimates in the range $\theta > \pi/4$. When crack density is large and the fluid bulk modulus is small, Thomsen's approximation underestimates the SV-velocity for all directions. The discrepancy becomes large as the crack density increases, or as the bulk modulus of the crack-filling fluid becomes small.

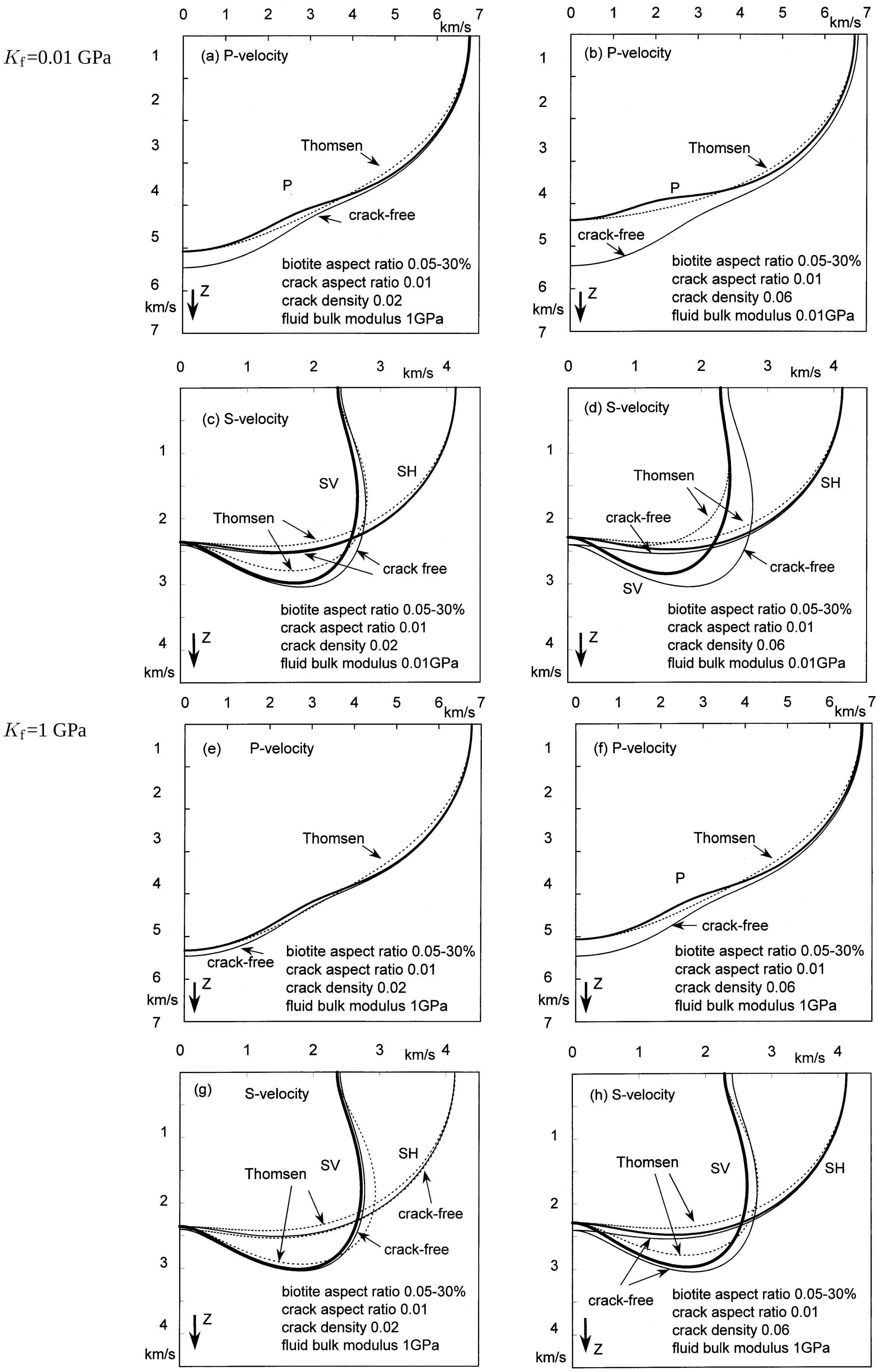

Fig. 1 Phase velocity surfaces of P-, SV-, and SH-waves for the rock containing 30% volume ratio of biotite and cracks with aspect ratio 0.01. The bulk modulus of crack-filling fluid is (a)-(d) 0.01 GPa, and (e)-(h) 1 GPa. The left column, (a), (c), (e) and (g) correspond to crack density 0.02. The right column, (b), (d), (f) and (h) correspond to crack density 0.06.

Laboratory velocity measurements of biotite schist

We made laboratory velocity measurements of Hidaka biotite schist under confining pressures up to 150 MPa. The rock was sampled from Hidaka metmorphic belt, Hokkaido, Japan, and shows foliation and lineation that is parallel to the foliation plane. The layering sheet of biotite crystals and the crack planes are mostly align parallel to the foliation plane. P- and the two polarized S-velocities were measured along the three axes: perpendicular to the foliation plane (z-axis) and the two direction in the foliation plane, parallel and perpendicular to the lineation (x- and y-axis, respectively). The polarization directions of the measured S-waves are located in the planes that are parallel or perpendicular to the symmetry axis.

The high pressure axial velocity values and the biotite LPO data indicate that anisotropy is basically TI but slightly shifts to orthorhombic because of slight misalignments of the layering sheets of biotite from the foliation plane in the y-direction (Takanashi et al., 2000). We approximate the anisotropy by a combination of two TI type anisotropy in the xz-plane and the yz-plane, both with the symmetry axis in the z-direction (Tsvankin 1997). Additional velocity measurements were made along the direction 45 degrees from the z-axis in the xz- and yz-planes for P-, SV- and SH-waves. We observed a bulge of SV-wave phase velocity in the xz-plane under high confining pressure. In the xz-plane, S-wave shows singularity (Takanashi et al., 2000).

Fig. 2 shows the changes of P- and S-velocities with respect to confining pressure. The P-velocity perpendicular to the foliation plane, (V_{Pz}), increases 1.5 km/s from atmospheric pressure to 150 MPa, whereas the P-velocity in the lineation direction, (V_{Px}), increases only 0.5 km/s in the same pressure interval. This suggests that the most cracks are aligned parallel to the foliation plane. The P-velocity along 45 degress from the z-axis, V_{Px45z} increases with increasing the confining pressure and become close to the V_{Pz} value under high pressures. This corresponds to the non-ellipticity of the intrinsic P-velocity of biotite-rich rock (Nishizawa and Yoshino, 2000; Takanashi et al., 2000). The S-velocities in the x- and z-directions change only little with increasing confining pressure, because effects of micro cracks on S-velocities are weak. V_{SVx45z} increases with increasing pressure, whereas V_{SHx45z} increases slightly below 40 MPa and becomes almost constant above 40 MPa. The difference betwenn V_{SVx45z} and V_{SHx45z} increases with increasing pressure. This phenomenon is interpreted as a coupled effect of the crack anisotropy and the intrinsic anisotropy of the biotite-rich rock.

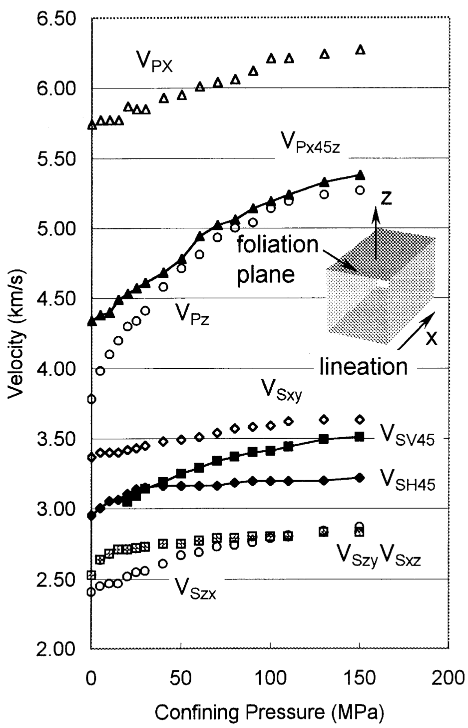

Fig. 2 Measured P- and S-velocities of the Hidaka biotite schist as a function of confining pressure. Velocities measured at the xz-plane are shown in the figure.

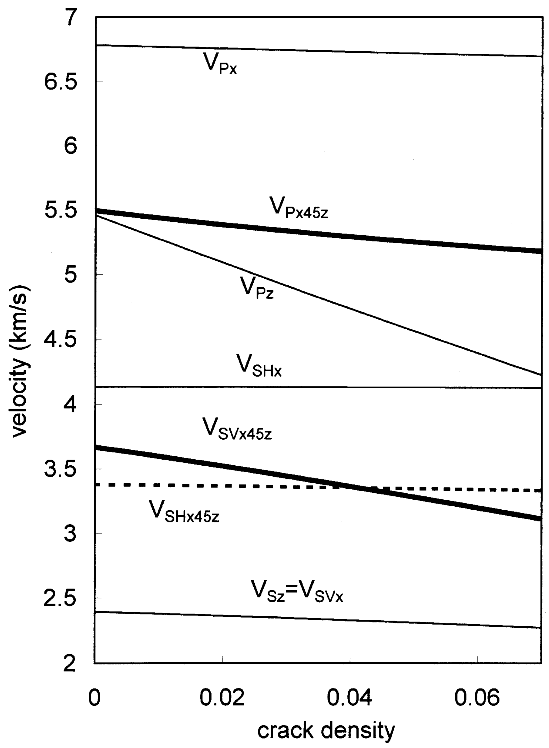

Fig. 3 P- and S-wave velocities as a function of crack density.

Discussion

We interpret the velocity change under confining pressure by an inclusion model where oriented cracks are aligned in a transversely isotropic matrix containing biotite crystals. Fig. 3 shows changes of the P-, SV- and SH-velocities with respect to the crack density. The velocities in the direction θ=45° (V_{Px45z}, V_{SVx45z} and V_{SHx45z}) are shown together with the velocities in the x- and z-directions. Crack density ε is defined by porosity ϕ and aspect ratio of crack α as

$$\varepsilon = 3\phi/4\pi\alpha \quad . \tag{15}$$

V_{Px45z} is not sensitive to crack density: the sensitivity is almost same as V_{Px}, although the absolute velocity value is smaller than V_{Px}. V_{SHx45z} is almost constant with respect to crack density. However, the V_{SVx45z} decreases with increasing crack density, and crosses the V_{SHx45z} at the crack density about 0.04. Since decrease of confining pressure is equivalent to increase of crack density, the calculated results agree with the experimental results. We conclude that the experimental results can be successfully interpreted by using a crack model having aligned cracks in the matrix of TI-type anisotropy containing aligned biotite crystals.

The bulge of SV-wave is important for analyzing the shear wave data. First, the bulge affects the group velocity of SV-wave, forming a cusp in the wave front (Banik, 1987; Hornby, 1994). The cusp will produce complicated waveforms and may cause serious problems for data analysis in seismic explorations. Second, the magnitude of SV-wave bulge is controlled mainly by the fluid bulk modulus. When the crack-filling fluid changes its phase, for example, from liquid to gas, a considerable change of the SV-velocity is expected in the directions around θ=45°. This will affect shear wave splitting, and may be important to monitor underground environments.

Conclusions

We have examined velocity anisotropy of a rock having oriented cracks in a strong TI anisotropic medium. The measured velocity under different confining pressure for Hidaka biotite schist can be successfully explained by closure of oriented cracks under confining pressure. The change of the bulge in the SV-phase velocity surface will affect interpretation of shear wave splitting or waveform analysis. The bulk modulus of the crack-filling material is an important factor that controls the velocity anisotropy.

Acknowledgments
We thank Prof. Tanio Ito for encouraging velocity measurements of the Hidaka metamorphic rocks.

References

Alekesandrov, K. S. & Ryzhova, T. V., 1961. The elastic properties of rock-forming minerals, Ⅱ: Layered silicates *Izv. Acad. Sci. USSR, Geophys. Ser.*, **12**, 186-189.

Banik, N. C., 1987. An effective anisotropy parameter in transversely isotropic media *Geophysics*, **52**, 1654-1664.

Crampin, S. & Yedlin, M. 1981. Shear-wave singularities of wave propagation in anisotropic media, *J. Geophys.*, **49**, 43-46.

Douma, J., 1988. The effect of the aspect ratio on crack-induced anisotropy, *Geophys. Prospecting*, **36**, 614-632.

Douma, J. & Crampin, S., 1990. The effect of a changing aspect ratio of aligned cracks on shear wave vertical seismic profiles: a theoretical study, *J. Geophys. Res.*, **95**, 11293-11300.

Eshelby, J., 1957. The determination of the elastic field of an ellipsoidal inclusion, and related problems, *Proc. Roy. Soc.*, **A241**, 376-396.

Hornby, B. E., Schawartz, L. M., & Hudson, J. A., 1994. Anisotropic effective-medium modelling of the elastic properties of shales, *Geophysics*, **59**, 1570-1583.

Le Ravalec, M., Gueguen, Y., 1996a. High and low frequency elastic moduli fora saturated porous/cracked rock (differential self consisitent and poroelastic theories), *Geophysics*, **61** 1080-1094,

Le Ravalec, M., Gueguen, Y., 1996b. Comments on ”The elastic modulus of media containing strongly interacting cracks” by Paul M. Davis and Leon Knopoff, *J. Geophys. Res.*, **101**, 25373-25375.

Lin, S. & Mura, T,. 1973. Elastic fields of inclusions in anisotropic media (Ⅱ), *Phys. Status Solidi*, **(a) 15**, 281-285.

Nishizawa, O., 1982. Seismic velocity anisotropy in a medium containing oriented cracks — Transversely isotropic case —, *J. Phys. Earth*, **30**, 331-347.

Nishizawa, O. & Yoshino, T., 2000. Seismic velocity anisotropy in mica-rich rocks: An inclusion model, *Geophys. J. Int., in print*

Singh, S. C., Taylor, M. A. J. & Montagner, J. P., 2000. On the presence of liquid in Earth's inner core, *Scinece*, **287**, 2471-2474.

Takanashi, M., Nishizawa, O., Kanagawa, K. & Yasunaga, K., 2000. Laboratory measurements of elastic anisotropy parameters for the exposed crustal rocks from Hidaka metamorphic belt, central Hokkaido, Japan, *Geophys. J. Int., in print*.

Thomsen, L., 1986. Weak elastic anisotropy, *Geophysics*, **51**, 1954–1966.

Tsvankin, I., 1997. Anisotropic parameters and *P*-wave velocity for orthorhombic media, *Geophysics*, **62**, 1292–1300.

Yamamoto, K., Kosuga, M., & Hirasawa, T., 1981. A theoretical method for determination of effective elastic constants of isotropic composite, *Sci. Rep. Tohoku Univ., Ser. 5*, **28**, 47-67.